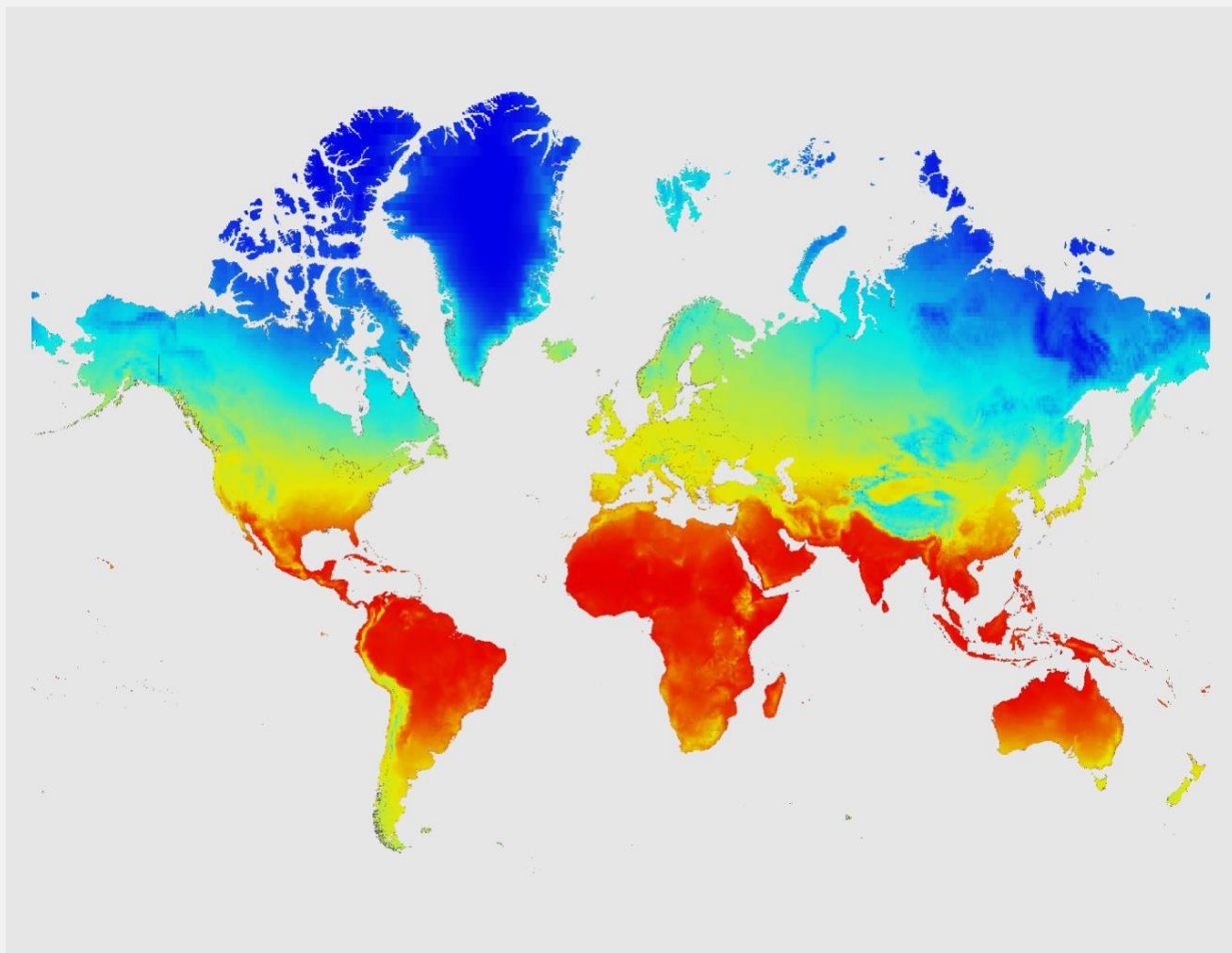


METADATA

CLIMATE CHANGE KNOWLEDGE PORTAL (CCKP)



© November 2021

TABLE OF CONTENTS

1. CLIMATE DATA	3
Observed, Historical Climate Data	3
Data Source: CRU TS v.4.05.....	3
Climate Projection Data.....	3
Data Source: CMIP6.....	4
Data Source: CMIP5.....	7
Essential Climate Variables	9
Climate Indicators	9
Data Processing Steps And Evaluation Protocol	13
CCKP Data Visualizations.....	16
2. VULNERABILITY	19
Natural Hazards Data.....	19
Global Risk Data Platform	20
Pacific Islands Hazards.....	20
EM-DAT	20
3. IMPACTS	21
Agriculture	21
Low/High Input, Irrigated/Rainfed Crops	21
Global Irrigated Areas Map	21
Global Map Of Rainfed Cropland Areas	22
Global Map Of Irrigation Areas	23
Harvested Area And Yields (M3-Crops Data).....	24
Water.....	24
Water Indicator	24
Aquastat	25
Sea Level	25
Historical Sea Level Anomaly	25
Observed Sea Surface Temperature	26
Sea Level Rise Projects.....	27

1. CLIMATE DATA

OBSERVED, HISTORICAL CLIMATE DATA

DATA SOURCE: CRU TS v.4.05

Citable as: Harris, I., Osborn, T.J., P. et al. Version 4 of the CRU TS monthly high-resolution gridded multivariate climate dataset. *Sci Data* 7, 109 (2020). <https://doi.org/10.1038/s41597-020-0453-3>

Data access:

<https://crudata.uea.ac.uk/cru/data/hrg/>

https://data.ceda.ac.uk/badc/cru/data/cru_ts/

CRU TS (Climatic Research Unit gridded Time Series) is the most widely used observational climate dataset. Data is presented on a 0.5° latitude by 0.5° longitude grid over all land domains except Antarctica. It is derived by the interpolation of monthly climate anomalies from extensive networks of weather station observations. The CRU TS version 4.05 gridded dataset is derived from observational data and provides quality-controlled temperature and rainfall values from thousands of weather stations worldwide, as well as derivative products including monthly climatologies and long term historical climatologies. The dataset is produced by the Climatic Research Unit (CRU) of the University of East Anglia (UEA).¹ To test the ability of models to represent the historical climate, simulations of that historical past (for the same period as the data available for CRU) are compared against CRU. To evaluate projected temperature and precipitation, the model's representation of the seasonal cycle (monthly values for key variables) is additionally evaluated with respect to historic values. The same thresholds and assumptions to categorize the observed changes have been used for the projected changes.

Observed, historical data is presented as distinct climatologies (the current climatology is 1991-2020) on CCKP, for geospatial analysis or through the seasonal cycle. The long-term time series shows observed data, 1901-2020.

CLIMATE PROJECTION DATA

Climate projection data presented on CCKP is derived from both the [CMIP5](#) and [CMIP6](#) (Coupled Inter-comparison Project, Phase 5 and Phase 6) collections. CMIP is a standard experimental framework for studying the output of coupled atmosphere-ocean general circulation models, overseen by the [World Climate Research Program](#). The CMIPs are designed to improve the understanding of past, present and future climate changes arising from natural, unforced variability or in response to changes in radiative forcing in a multi-model context. This understanding includes assessments of model performance during the historical period and quantifications of the causes of the spread in future projections. Idealized experiments are also used to increase understanding of the model responses. In addition to these long-time scale responses, experiments are performed to investigate the predictability of the climate system on various temporal and spatial scales as well as making predictions from observed climate states. Modeled climate data is presented as a 1.0° latitude by 1.0° longitude grid, produced through bi-linear interpolation.

¹ University of East Anglia. 2020: Climatic Research Unit. URL: <http://www.cru.uea.ac.uk/about-cru>

DATA SOURCE: CMIP6

Original source data: The Coupled Model Intercomparison Project, v. 6 – CMIP6: Eyring, V., Bony, S., Meehl, G. A., Senior, C. A., Stevens, B., Stouffer, R. J., and Taylor, K. E., 2016: Overview of the Coupled Model Intercomparison Project Phase 6 (CMIP6) experimental design and organization, *Geosci. Model Dev.*, 9, 1937–1958, DOI: <https://doi.org/10.5194/gmd-9-1937-2016>

Data access:

<https://www.wcrp-climate.org/wgcm-cmip/wgcm-cmip6>

<https://pcmdi.llnl.gov/CMIP6/Guide/dataUsers.html>

CMIP6 model output is structured similar to CMIP5 output, but changes have been made to accommodate the more complex structure of CMIP6 and its data request.

The scenario approach is used to characterize the range of plausible climate futures and to illustrate the consequences of different pathways. The scenarios are chosen to span a wide range without any tie to likelihood. Over the past three decades, the approach to formulating the different ‘scenarios’ has evolved from a climate-centric to an increasingly societal development -centric concept, albeit with the same underlying goal of providing insight into a range of plausible climate outcomes. CMIP6 presents scenarios as the Shared Socioeconomic Pathways (SSPs), instead of the RCPs used in CMIP6. CMIP6 climate projections are driven by a new set of emissions and land use scenarios produced with integrated assessment models (IAMs) based on new future pathways of societal development, the SSPs, and related to the RCPs.² While outputs are similar, CMIP6 climate projections will differ from those in CMIP5 not only because they are produced with updated versions of climate models, but also because they are driven with SSP-based scenarios produced with updated versions of IAMs and based on updated data on recent emissions trends. Unlike in CMIP3 and CMIP5, where climate model projections were part of the core experiments, in CMIP6 they are part of a dedicated CMIP6-Endorsed MIP.³

CMIP6 present five primary scenarios, which represent *possible* societal development and policy paths for meeting designated radiative forcing by the end of the century. These represent *possible* societal development and policy paths for meeting designated radiative forcing by the end of the century and were not meant to be interpreted as the only possible path to get to the specific forcing levels. **SSP1-1.9** presents the most optimistic scenario and was added to offer insight into the insight into the climate response that might be reflective of the Paris-Accord target and presents a radiative forcing of 1.9W/m² by 2100. **SSP1-2.6** supports increasing sustainability with global emissions cut severely, but reach net-zero after 2050. **SSP2-4.5** presents a ‘middle of the road’ scenario in which emissions remain around current levels, before starting to fall around mid-century, but do not reach net-zero by 2100. **SSP3-7.0** presents a pathway in which countries are increasingly competitive and emissions continue to climb, roughly doubling from current levels by 2100. **SSP5-8.5** presents

² O'Neill, B. C., Tebaldi, C., van Vuuren, D. P., Eyring, V., Friedlingstein, P., Hurtt, G., Knutti, R., Kriegler, E., Lamarque, J.-F., Lowe, J., Meehl, G. A., Moss, R., Riahi, K., and Sanderson, B. M., 2016: The Scenario Model Intercomparison Project (ScenarioMIP) for CMIP6, *Geosci. Model Dev.*, 9, 3461–3482, <https://doi.org/10.5194/gmd-9-3461-2016>.

³ Eyring, V., Bony, S., Meehl, G. A., Senior, C. A., Stevens, B., Stouffer, R. J., and Taylor, K. E., 2016: Overview of the Coupled Model Intercomparison Project Phase 6 (CMIP6) experimental design and organization, *Geosci. Model Dev.*, 9, 1937–1958, DOI: <https://doi.org/10.5194/gmd-9-1937-2016>

a future based on an intensified exploitation of fossil fuel resources where global markets are increasingly integrated leading to innovations and technological progress.

CMIP6 model data is licensed under a [Creative Commons Attribution-ShareAlike 4.0 International License](#). See [terms of use governing CMIP6 output](#), including citation requirements and proper acknowledgment. Further information about this data, including some limitations, can be found via the further_info_url (recorded as a global attribute in the netCDF files). The data producers and data providers make no warranty, either express or implied, including, but not limited to, warranties of merchantability and fitness for a particular purpose. All liabilities arising from the supply of the information (including any liability arising in negligence) are excluded to the fullest extent permitted by law.

We acknowledge the World Climate Research Programme, which, through its Working Group on Coupled Modelling, coordinated and promoted CMIP6. We thank the climate modeling groups for producing and making available their model output, the Earth System Grid Federation (ESGF) for archiving the data and providing access, and the multiple funding agencies who support CMIP6 and ESGF.

We also extend our thanks to the CMIP6ng effort at ETH-Zuerich, Switzerland from where some daily data has been acquired: ETH Zurich CMIP6 "next generation" (ng) archive.⁴

The CCKP-CMIP6 collection consists of up to 31 models (**Table 1**) that submitted data across the SSPs. All data was processed using the Climate Risk Management engine (CRMe) infrastructure⁵ (Ammann et al. 2016) and formatted using ArcGIS and functions offered through the Open Geospatial Consortium (<http://www.opengeospatial.org/>).

Table 1. List of models used in CCKP CMIP6 compilation

Model Name on CCKP	Modeling Center	Responsible Institution
ACCESS-CM2	CISRO-ARCCSS	CSIRO (Commonwealth Scientific and Industrial Research Organization, Australia), and ARCCSS (Australian Research Council Centre of Excellence for Climate System Science)
ACCESS-ESM1-5	CISRO	CSIRO (Commonwealth Scientific and Industrial Research Organization, Australia)
AWI-CM-1-1-MR	AWI	Alfred Wegener Institute
BCC-CSM2-MR	BCC	Beijing Climate Center
CAMS-CSM1-0	CAMS	Chinese Academy of Meteorological Sciences

⁴ Brunner L., M. Hauser, R. Lorenz, and U. Beyerle (2020). The ETH Zurich CMIP6 next generation archive: technical documentation. DOI:[10.5281/zenodo.3734128](https://doi.org/10.5281/zenodo.3734128). URL: <https://zenodo.org/record/3734128#.YYgKbS-B2X0>. This dataset is provided "as is", without warranty of any kind. The ownership of this dataset remains with the original provider.

⁵ Ammann et al. 2016: An Efficient Workflow Environment to Support the Collaborative Development of Actionable Climate Information Using the NCAR Climate Risk Management Engine (CRMe). AGU Fall Meeting. 12 December, 2016. URL: <https://agu.confex.com/agu/fm16/meetingapp.cgi/Paper/197594>

CANESM5	CCCma	Canadian Centre for Climate Modelling and Analysis
CESM2	NCAR	National Center for Atmospheric Research
CMCC_CM2-SR5 CMCC-ESM2	CMCC	Euro-Mediterranean Center on Climate Change
CNRM-CM6-1	CNRM	Centre National de Recherches Meteorologiques
CNRM-ESM2-1	CNRM-CERFACS	Centre National de Recherches Meteorologiques / Centre Européen de Recherche et Formation Avancées en Calcul Scientifique
EC-EARTH3 EC-EARTH3-VEG	EC-Earth- Consortium	EC-Earth-Consortium: La Agencia Estatal de Meteorología (AEMET), Barcelona Supercomputing Centre (BSC), Institute of Atmospheric Sciences and Climate (CNR-ISAC), Danish Meteorological Institute (DMI), Italian National Agency for New Technologies, Energy and Sustainable Economic Development (ENEA), Finnish Meteorological Institute (FMI), Helmholtz Centre for Ocean Research Kiel (Geomar), Irish Centre for High-End Computing (ICHEC), International Centre for Theoretical Physics (ICTP), Instituto Dom Luiz (IDL), Institute for Marine and Atmospheric research Utrecht (IMAU), Portuguese Institute for Sea and Atmosphere (IPMA), KIT Karlsruhe Institute of Technology, Royal Netherlands Meteorological Institute (KNMI), Lund University, Met Eireann, The Netherlands eScience Center (NLeSC), Norwegian University of Science and Technology (NTNU), University of Oxford, SURFsara, Swedish Meteorological and Hydrological Institute (SMHI), Stockholm University, Unite ASTR, University College Dublin, University of Bergen, University of Copenhagen, University of Helsinki, University of Santiago de Compostela, Uppsala University, University of Utrecht, Vrije Universiteit Amsterdam and Wageningen University.
FGOALS-G3	CAS	China Academy of Sciences
GFDL_ESM4	NOAA GFDL	Geophysical Fluid Dynamics Laboratory
HADGEM3-GC31-II	MOHC-NERC	UK Met Office Hadley Centre
INM-CM4-8 INM-CM5-0	INM	Institute for Numerical Mathematics
IPSL_CM6A_LR	IPSL	The Institute Pierre Simon Laplace
KACE-1-0-g	NIMS-KMA	National Institute of Meteorological Sciences (SIMS) and Korea Meteorological Administration (KMA)
KIOST-ESM	KIOST	Korea Institute of Ocean Science and Technology
MIROC-ES2I MIROC6	MIROC	Atmosphere and Ocean Research Institute (The University of Tokyo), Center for Climate system Research - National Institute for Environmental Studies
MPI_ESM1-2-HR	MPI-M DWD DKRZ	Max Planck Institute for Meteorology (MPI-M)
MPI-ESM1-2-LR MRI-ESM2	MRI	Meteorological Research Institute

NESM3	NUIST	Nanjing University of Information Science and Technology
NORESM2-LM	NCC	Norwegian Climate Centre
NORESM2-MM		
TAIESM1	AS-RCEC	Research Center for Environmental Changes, Academia Sinica
UKESM1-0-II	MOHC NERC NIMS-KMA NIWA	National Institute of Meteorological Sciences, Korea Meteorological Administration-Climate Research Division

DATA SOURCE: CMIP5

Original source data: The Coupled Model Intercomparison Project, v. 5 – CMIP5: Taylor, K. E., R. J. Stouffer, and G. A. Meehl, 2012: An Overview of CMIP5 and the Experiment Design. *B Am Meteorol Soc*, 93, 485-498. DOI: <https://doi.org/10.1175/BAMS-D-11-00094.1>

Data access:

<https://www.wcrp-climate.org/wgcm-cmip/wgcm-cmip5>

<https://pcmdi.llnl.gov/mips/cmip5/>

The CMIP5 experiment design was finalized with the following suite of experiments:

- 1) Decadal Hindcasts and Predictions simulations;
- 2) "Long-term" simulations; and
- 3) "Atmosphere-only" (prescribed SST) simulations for especially computationally demanding models.

Future climates are represented through different possible future radiative forcing scenarios. Four [Representative Concentration Pathways](#) (RCPs) were developed by the Intergovernmental Panel on Climate Change (IPCC) and are used to make projections based on anthropogenic GHG emissions, which are driven primarily by population size, economic activity, lifestyle, energy use, land use patterns, technology and climate policy. The RCPs describe different 21st century pathways of GHG emissions and atmospheric concentrations, air pollutant emissions, and land use. The RCPs include a stringent mitigation scenario (**RCP2.6**), two intermediate scenarios (**RCP4.5** and **RCP6.0**) and one scenario with very high GHG emissions (**RCP8.5**). Scenarios without additional efforts to constrain emissions ('baseline scenarios') lead to pathways ranging between RCP6.0 and RCP8.5.⁶ The RCPs represent the global mean radiative forcing in watts per square-meter (W/m^2) achieved in each of the scenarios by the year 2100.

The CCKP-CMIP5 collection consists of up to 35 models (**Table 2**) that submitted data across the RCPs and for which the data were readily available over the Earth System Grid Federation. The data used here were obtained through the IPCC Working Group I data snapshot, offered by the Swiss Federal Technical University in Zürich (ETHZ)⁷ (thanks to U. Beyerle). All data was processed using the Climate Risk Management engine

⁶ Previously (up to CMIP3), these scenarios were called emission scenarios as presented in the Special Report on Emission Scenarios – SRES scenarios A2, A1FI, A1B, B1.

⁷ Emori, S., Taylor, K., Hewitson, B., Zermoglio, F., Jukes, M., Lautenschlager, M. and Stockhause, M. 2016: *CMIP5 data provided at the IPCC Data Distribution Centre*. Fact Sheet of the Task Group on Data and Scenario Support for Impact

(CRMe) infrastructure⁸ (Ammann et al. 2016) and formatted using ArcGIS and functions offered through the Open Geospatial Consortium (<http://www.opengeospatial.org/>).

Table 2. List of models used in CCKP compilation

Model Name on CCKP	Modeling Center	Responsible Institution
ACCESS1_0	CSIRO-BOM	CSIRO (Commonwealth Scientific and Industrial Research Organization, Australia), and BOM (Bureau of Meteorology, Australia)
ACCESS1_3		
BCC_CSM1_1 ^{ECV}	BCC	Beijing Climate Center, China Meteorological Administration
BCC_CSM1_1_M ^{ECV}		
BNU_ESMU_ESM	GCESS	College of Global Change and Earth System Science, Beijing Normal University
CANESM2	CCCma	Canadian Centre for Climate Modelling and Analysis
CCSM4 ^{ECV}	NCAR	National Center for Atmospheric Research
CESM1_BGC	NSF-DOE-NCAR	National Science Foundation, Department of Energy, National Center for Atmospheric Research
CESM1_CAM5 ^{ECV}		
CMCC_CESM	CMCC	Euro-Mediterranean Center on Climate Change
CMCC_CM		
CMCC-CMS		
CNRM-CM5	CNRM-CERFACS	Centre National de Recherches Meteorologiques / Centre Européen de Recherche et Formation Avancées en Calcul Scientifique
CSIRO_MK3_6_0 ^{ECV}	CSIRO-QCCCE	Commonwealth Scientific and Industrial Research Organization in collaboration with the Queensland Climate Change Centre of Excellence
FIO_ESM ^{ECV}	FIO	The First Institute of Oceanography, SOA, China
GFDL_CM3 ^{ECV}	NOAA GFDL	Geophysical Fluid Dynamics Laboratory
GFDL_ESM2G		
GFDL_ESM2M ^{ECV}		
GISS_E2_H ^{ECV}	NASA GISS	NASA Goddard Institute for Space Studies
GISS_E2_R ^{ECV}		
HADGEM2_CC	MOHC (additional realizations by INPE)	Met Office Hadley Centre (additional HadGEM2-ES realizations contributed by Instituto Nacional de Pesquisas Espaciais)
HADGEM2_ES		
HADGEM2_AO	NIMR/KMA	National Institute of Meteorological Research/Korea Meteorological Administration
INMCM4	INM	Institute for Numerical Mathematics

and Climate Analysis (TGICA) of the Intergovernmental Panel on Climate Change (IPCC), 8 pp. URL: https://www.ipcc-data.org/docs/factsheets/TGICA_Fact_Sheet_CMIP5_data_provided_at_the_IPCC_DDC_Ver_1_2016.pdf

⁸ Ammann et al. 2016: An Efficient Workflow Environment to Support the Collaborative Development of Actionable Climate Information Using the NCAR Climate Risk Management Engine (CRMe). AGU Fall Meeting, 12 December, 2016. URL: <https://agu.confex.com/agu/fm16/meetingapp.cgi/Paper/197594>

IPSL_CM5A_LR	IPSL	The Institute Pierre Simon Laplace
IPSL_CM5A_MR ^{ECV}		
IPSL_CM5B_LR		
MIROC_ESM ^{ECV}	MIROC	Japan Agency for Marine-Earth Science and Technology, Atmosphere and Ocean Research Institute (The University of Tokyo), and National Institute for Environmental Studies
MIROC_ESM_CHEM ^{ECV}		
MIROC5 ^{ECV}	MIROC	Atmosphere and Ocean Research Institute (The University of Tokyo), National Institute for Environmental Studies, and Japan Agency for Marine-Earth Science and Technology
MPI_ESM_LR	MPI-M	Max Planck Institute for Meteorology (MPI-M)
MPI_ESM_MR		
MRI_CGCM3 ^{ECV}	MRI	Meteorological Research Institute
MRI_ESM1		
NORESM1_M ^{ECV}	NCC	Norwegian Climate Centre

* **ECV**: Essential Climate Variables

For each model, a section of the *historical* simulations was required to form each model's own reference period. While generally the World Meteorological Organization prefers reference periods that span 30 years (e.g., 1971-2000, or 1981-2010), the IPCC-AR5 (Stocker et al. 2013) broadly utilized a **20-year interval of 1986-2005(CMIP5)** and **1995-2014(CMIP6)**. This period covers the final 20 years of the *historical* simulations that were driven with observed radiative forcings. A 20-year window also corresponds to the CCKP requested 20-year climatological windows for the future, **specific time periods: 2020-2039, 2040-2059, 2060-2079, and 2080-2099**. For each of these future time windows, simulations from all four RCPs and five SSPs were obtained and processed for **4 essential climate variables** and **additional derived climate indices (Table 3)**.

ESSENTIAL CLIMATE VARIABLES

The essential climate variables of temperature (mean, min and max) and precipitation were produced with the objective of providing the most robust comparison between different RCPs and SSPs possible. They were processed separately from the climate indicators. This most basic climate change projection information was restricted to a fixed collection of models that required that information was available for all of the different RCPs or SSPs, and therefore a direct comparison between RCPs and between SSPs is most robust.

CLIMATE INDICATORS

Climate indicators capture a specific characteristic of weather and climate that can have more specific impacts on the ground. CCKP offers multiple indicators (**Table 3**), which consist of a subset of the climate statistics indicators from the joint CCI/CLIVAR/JCOMM Expert Team on Climate Change Detection and Indices (ETCCDI) (see: http://etccdi.pacificclimate.org/list_27_indices.shtml) and others developed during this project specifically to meet sectoral needs or requests (particularly return intervals and drought indicators).⁹

⁹ The precipitation return interval calculations are based on the automatic algorithm of Naveau et al. 2016 (Modeling jointly low, moderate, and heavy rainfall intensities without a threshold selection, Water Resour. Res., 52, 2753– 2769,

CCKP presents all projection indicators as mean or as anomaly (from the Historical Reference Period: 1986-2005 for CMIP5) and (from the Historical Reference Period: 1995-2014 for CMIP6), with data provided at annual, monthly or seasonal scales, and as climatology, timeseries, heatmap or global-gridded NetCDF files for geospatial data.

All temperature base series were bias corrected at the annual mean level of the climatology over the baseline period. Derived indices, such as number of days with temperatures above 35°C or 40°C and heat indices are highly sensitive to the absolute temperature and moisture, and thus benefit from such a bias correction. However, due to lack of good observational data and because of much larger challenges in representing this component, rainfall and humidity have not been adjusted to prevent unphysical outcomes.

Table 3. List of climate indicators

No.	Variable Name	Unit	Description
ESSENTIAL CLIMATE VARIABLES			
1	Max-Temperature	°C	Average maximum-temperature.
2	Mean Temperature	°C	Average mean temperature.
3	Min-Temperature	°C	Average minimum-temperature.
4	Precipitation	°C	Precipitation, sum over identified period.
TEMPERATURE-RELATED FIELDS			
5	Cold Spell Duration Index	Days	Number of days that are part of a sequence of 6 or more days in which the daily minimum temperature exceeds the 10 th percentile of the reference period.
6	Cooling Degree Days (ref 65°F)	°C	Number of degrees that a day's average temperature is above 18.3°C.
7	Daily Probability of Cold Wave	Probability	The daily probability of observing a cold wave, which is a 3 or more-day sequence where the daily temperature is below the long-term 5 th percentile of daily mean temperature.
8	Daily Probability of Heat Wave	Probability	The daily probability of observing a heat wave, which is a 3 or more-day sequence where the daily temperature is above the long-term 95 th percentile of daily mean temperature.

doi:10.1002/2015WR018552) that does not require local *a priori* specification of a threshold beyond which precipitation would be considered as distributed following an extreme value distribution. The results presented thus far are the mean expected outcome

9	Growing Season Length	Days	Number of days between the first and last period of 6 or more consecutive days with a daily mean temperature above 5°C
10	Heating Degree Days (ref 65°F)	°C	Number of degrees that a day's average temperature is below 18.3°C.
11	Maxima of Daily Max-Temperature	°C	Maximum of daily max-temperature per month or year.
12	Minima of Daily Min-Temperature	°C	Minimum of daily min-temperature per month or year.
13	Number of Days with Dangerous Heat (Heat Index > 35°C)	Days	Average count of days when the daily Heat Index surpassed 35°C.
14	Number of Excessively Hot Days (Tmax > 45°C)	Days	Average count of days when the maximum temperature surpassed 45°C.
15	Number of Extremely Hot Days (Tmax > 40°C)	Days	Average count of days when the maximum temperature surpassed 40°C.
16	Number of Extremely Hot Days (Tmax > 42°C)	Days	Average count of days when the maximum temperature surpassed 42°C.
17	Number of Frost Days (Tmin < 0°C)	Days	Average count of days when the minimum temperature dropped below the freezing point of water at 0°C.
18	Number of Hot Days (Tmax > 30°C)	Days	Average count of days when the maximum temperature surpassed 30°C.
19	Number of Ice Days (Tmax < 0°C)	Days	Average count of days when the daily maximum temperature did not break through the freezing point but remained below 0°C.
20	Number of Summer Days (Tmax > 25°C)	Days	Average count of days where the daily maximum temperature surpassed 25°C.
21	Number of Tropical Nights (Tmin > 20°C)	Days	Average count of days where the daily minimum temperature remained above 20°C.
22	Number of Tropical Nights (Tmin > 26°C)	Days	Average count of days where the daily minimum temperature remained above 26°C.
23	Number of Very Hot Days (Tmax > 35°C)	Days	Average count of days when the maximum temperature surpassed 35°C.
24	Warm Spell Duration Index	Days	Number of days that are part of a sequence of 6 or more days in which the daily maximum temperature exceeds the 90 th percentile of the reference period.
MOISTURE-RELATED FIELDS			
25	Annual Probability for experiencing a year with Severe Drought conditions	SPEI Index	The annual probability of experiencing Severe medium-term drought, determined by the Standardized Precipitation Evaporation Index (using 12-month window, where SPEI is computed over the full period, with threshold for severe drought at -2)

26	Days with Precipitation >10mm	Days	Average count of days with at least 10 mm of daily precipitation
27	Expected Daily Precipitation Maximum in 10 Years (10-yr Return Level)	mm	Statistical 10-yr return level of the largest daily precipitation event.
28	Expected 5-day Cumulative Precipitation Maximum in 10 Years (10-yr Return Level)	mm	Statistical 10-yr return level of the largest 5-day consecutive precipitation sum.
29	Expected Daily Precipitation Maximum in 25 Years (25-yr Return Level)	mm	Statistical 25-yr return level of the largest daily precipitation event.
30	Expected 5-day Cumulative Precipitation Maximum in 25 Years (25-yr Return Level)	mm	Statistical 25-yr return level of the largest 5-day consecutive precipitation sum.
31	Expected Largest Monthly Precipitation Amount in 10 Years (10-yr Return Level)	mm	Statistical 10-yr return level of the largest monthly rainfall sum.
32	Expected Largest Monthly Precipitation Amount in 25 Years (25-yr Return Level)	mm	Statistical 25-yr return level of the largest monthly precipitation sum.
33	Largest 5-day Cumulative Precipitation	mm	Average of the largest 5-day consecutive precipitation amount.
34	Largest Single Day Precipitation	mm	Average of the largest daily precipitation amount.
35	Maximum Length of Consecutive Dry Spell	Days	Number of days in the longest period without significant precipitation of at least 1mm.
36	Maximum Length of Consecutive Wet Spell	Days	Number of days in the longest period with continuous significant rainfall of 1mm or more.
37	Mean Drought Index	SPEI-12	Changes in the mean of 12-month cumulative water balance, taking into account evapotranspiration.
38	Number of Days with Precipitation > 20mm	Days	Average count of days with at least 20mm of daily precipitation.
39	Number of Days with Precipitation > 50mm	Days	Average count of days with at least 50mm of daily precipitation.
40	Number of Wet Days	days	The number of wet days, or days in which the daily accumulated precipitation is 1mm
41	Precipitation Amount due to Extremely Wet Days	mm	The accumulated precipitation amount during the 1% wettest days over the data period
42	Precipitation Amount from Very Wet Days	mm	Monthly or annual sum of precipitation when the daily precipitation rate exceeds the local 95 th percentile of daily precipitation intensity.

43	Rainfall Seasonality	Standard Deviation	Standard deviation of monthly precipitation against the mean monthly rainfall across the year.
44	Range between Wettest and Driest Year	mm	The precipitation range between the driest and the wettest year over the period.
45	Total Precipitation, Percent Change	%	Projected total precipitation, anomaly shown as a percentage.
46	Total Precipitation from Wet Days	Mm	The total precipitation of wet days during the data period (wet day defined as any day in which the daily accumulated precipitation >1 mm)
OTHER			
47	Number of Days without Noticeable Wind	Days	Number of days where the mean wind speed is below 1 m/s.

DATA PROCESSING STEPS AND EVALUATION PROTOCOL

Essential Climate Variables

CMIP5 and CMIP6 model simulations were processed individually to establish a common dataset for which both absolute climatologies for the present and future 20-year intervals (2020-2039, 2040-2059, 2060-2079, and 2080-2099), as well as their relative changes in comparison to their common reference period of 1986-2005 or 1995-2014, respectively, could be computed. While the base-data was obtained as monthly time series, the products were to represent 20-year climatologies. Because of internal climate variability, the 20-year intervals at the grid level (or at aggregation levels of relatively small domains) become more useful when looking at the progressive changes throughout the 21st century with its continuously shifting climate. Each 20-year time window can therefore be compared to the standard “present day” reference period of 1986-2005 (CMIP5) or 1995-2014 (CMIP6). The resulting anomalies also correspond well to results presented in the IPCC.^{10,11} All models used in the calculations had to offer exactly the same suite of experiments and represented time periods.

Derived Indicators

Sector-oriented climate indicators often build on daily rather than monthly data. A collection of daily model output was processed for input into calculation of the climate indicators. Depending on the indicator, monthly, seasonal, and/or annual were generated for the RCPs and SSPs and time intervals for the basic climate fields. Some GCM and/ or IAM groups did not store or report humidity, pressure or wind fields on a daily basis, and thus not all indicators could be computed for all models. Therefore, in contrast to the basic climate fields, there are different numbers of models that contributed to the various ensembles at the level of the climate indicators.

¹⁰ Stocker, T. et al, (2013). Climate Change 2013 – The Physical Science Basis. Working Group I Contribution to the Fifth Assessment Report of the IPCC. URL: https://www.ipcc.ch/site/assets/uploads/2017/09/WG1AR5_Frontmatter_FINAL.pdf

¹¹ IPCC, 2021: Summary for Policymakers. In: Climate Change 2021: The Physical Science Basis. Contribution of Working Group I to the Sixth Assessment Report of the Intergovernmental Panel on Climate Change. Masson-Delmotte, V., P. et al. Cambridge University Press. In Press. URL: https://www.ipcc.ch/report/ar6/wg1/downloads/report/IPCC_AR6_WGI_Full_Report.pdf

This can introduce some inconsistencies when comparing different scenarios, though the direction and even the relative magnitude of the changes should still be useful.

The following steps describe how each of the models (listed in Table 3) were processed:

- a. **Re-gridding:** Initially, because all original model output is offered on their own native grids, the multi-model collection needed to be re-gridded to a common resolution. In order not to imply a false promise of high-resolution content in the GCM data, a common 1°x1° global grid spacing was produced through bi-linear interpolation. All analyses and data products within the CCKP distributions exclusively utilize these re-gridded data.
- b. **Climatologies:** For each model, and for each of the four selected essential climate variables, 20-year climatologies were formed. For CMIP5, the 'baseline' interval (1986-2005) was derived from the *historical* simulations ("*hist*"), while the future climatologies (2020-2039, 2040-2059, 2060-2079, 2080-2099) were computed for all four RCPs ("RCP2.6", "RCP4.5", "RCP6.0", "RCP8.5"). For CMIP6, the 'baseline' interval (1995-2014) was derived from the *historical* simulations ("*hist*"), while the future climatologies (2020-2039, 2040-2059, 2060-2079, 2080-2099) were computed for all five SSPs ("SSP1-1.9", "SSP1-2.6", "SSP2-4.5", "SSP3-7.0", "SSP5-8.5"). These climatologies consist of 12 monthly average values, 4 seasonal average values, and one annual mean value established over the respective time windows (sums for precipitation). To form the climatologies, all values were computed directly from the absolute temperature and precipitation data taken from the model simulations. Note, each model might exhibit slightly different absolute temperatures and precipitation. These offsets compared to observational data are generally small, yet in some regions they can be significant. In fact, because of these offsets in the depiction of climate in absolute values, the climatologies don't lend themselves easily for model-to-model intercomparisons of change. Better suited are comparisons of relative changes.
- c. **Bias Correction:** Because derived indicators can be very sensitive to errors in the data, particularly when looking at absolute thresholds (e.g., number of days with daily maximum temperatures above 40°C), a simple bias correction step was performed on the model's temperature data using the CRU-TS3.24 data (Harris and Jones, 2014), as the observational baseline. Each model's mean temperature was adjusted by the bias in their annual mean. For precipitation, this correction was not performed because of large uncertainties across the different gridded observational dataset that are available. For the temperature part, this bias correction is removing the first order discrepancies between models and observations during the historical periods. Such differences result from different choices and tuning across the models. Generally, the relative changes are regarded as more robust than the absolute temperatures which might be biased due to slight differences in geopotential height, land surface conditions (albedo), or other factors. After bias correction, the divergence between different model responses is clearly seen for the future periods. However, there are also some drawbacks. A few indicators, and particularly in most extreme climates, such as the polar regions, can at times exhibit unrealistic responses. For example, *because of the commonly large systematic errors in reproducing the extremely cold Antarctic interiors, the annual mean bias correction can sometimes lead to unrealistic values. In temperate and tropical regions, these errors are much smaller or nearly absent.*
- d. **Anomalies:** For each model, each variable, and for each of the four future time windows, anomalies for each month as well as the annual value were computed and assessed relative to their corresponding *historical* reference period. In contrast to the climatologies, these values are well suited for model-to-model intercomparisons as they always refer to the change simulated by each model.

Prior bias correction only is important for a few indicators that represent departures or counts above absolute thresholds (for example the number for days with minimum nighttime temperatures above 20°C).

- e. Ensemble Information: Ensemble values were calculated from the anomalies from each of the models in the collection, and for every 20-year climatological period in the future. These ensembles describe how the collection of up to 35 CMIP5 models and 31 CMIP6 models, on average, project the climatological changes. Different ways of exploring the ensemble distribution are possible. Here, the choice was done to use the median across the individual model values as the main representation. Next to that central value of the ensemble, also ensemble high (90th percentile) and low (10th percentile) values for all the climatological anomalies were generated to help users recognize the range of likely outcomes driven by the different sources of uncertainty. But values are available for each model separately, and thus the user could explore the distribution in more detail. Because each model has slightly different climate sensitivity and simulated different internal climate variability, the projections increasingly diverge into the future. Therefore, the ensemble spread generally increases with time. Note, each individual model's anomalies can be compared with the provided ensemble description that encompasses the range between high (90th percentile) and low (10th percentile) levels of the underlying distribution.

(**Note:** the number of available models may vary for different climate indicators. For example, the ensemble of tropical nights is calculated using 32 out of 35 models from the collection.)

- f. Climatological Ensemble Based on Observational Basis: A second ensemble product is provided as a condensed climatological description in absolute values of the projected changes across the multi-model collection. This ensemble is the combination of the absolute values from a common observational baseline dataset and the superposed multi-model ensemble anomalies (note, only the ensemble quantities are used, not each model's climatologies). The result is a description in absolute units of projected future climate as represented by the 90th percentile, the median (the 50th percentile), and the 10th percentile series. For the essential climate variables, these ensemble values were derived from the contributing models that reported all RCPs or SSPs, and in case of the sectoral indicators the values were established from across up to the full model distributions. In each case, the baseline was taken from the University of East Anglia, Climatic Research Unit (CRU) Time Series (TS) globally gridded dataset that was re-gridded to the same 1°x1° grid as the CMIP5 and CMIP6 data using bi-linear interpolation.

The intent of this ensemble is to provide users a condensed perspective in absolute values of projected future climate with its most faithful representation of uncertainty. Because individual models might potentially exhibit substantial biases, this composite approach of an ensemble characterization is significantly more useful for projecting the future climate than a direct ensemble visualization generated on the raw climatologies of each of the individual climate models. *Because of the biases, it is not recommended to plot the individual raw, absolute model climatologies together with the condensed ensemble ranges. Equally, just plotting the individual climatologies and forming an "on-the-fly" ensemble is not meaningful because the majority of differences (spread) is based simply on biases in each of the individual climate models and not a faithful representation of the true physical uncertainty.*

- g. Quality Control: Due to the large data volumes, not every field individually could be inspected visually. Rather, the CCKP Team implemented an automated final quality control algorithm on the publication-ready data to identify odd outliers in both absolute and anomaly fields. Suspicious values and

potentially suspicious model simulations were flagged and ultimately 4 models were excluded from the results. Once implemented into the CCKP, thorough visual inspection was performed to identify any remaining issues.

CCKP DATA VISUALIZATIONS

Geospatial Presentation (Maps)

Maps show the geospatial expression of different climate fields. Globally, temperature change varies primarily by latitude and elevation, but proximity to oceans also moderate this. Due to the absence of sunlight in winters, seasonality is particularly high in polar regions, and also increases in the interiors of continents. In the tropics, seasonality is minimized and often more easily recognizable through precipitation (e.g. a rainy and a dry season). However, the lack of strong seasonal oscillations and often a muted year-to-year variability causes the tropics to be much more sensitive to changes than areas at higher latitudes where ecosystems are used to large intra- and inter-annual variations so that small changes in temperature have often quite small environmental impacts.

While temperatures vary spatially only gradually (or due to topography), precipitation is often highly variable. This is often caused by the fact that precipitation is not a “continuous” field but represents intermittent processes with rainfall only occurring occasionally (with a few exceptions). Daily cycles as well as seasonal shifts of zones where precipitation occurs more systematically often lead to complex and often, quite strongly varying fields over a range of time scales. The only locations where precipitation is more regular is in the inner tropics as well as on the windward side of mountain ranges where orographic lift leads to condensation and precipitation. Therefore, maps of precipitation are often much less smooth than temperature or other fields, even when looking at climatologies that average precipitation over 20 or 30 years.

These general differences between temperature- and moisture-related fields can also be observed at the level of climate indicators. However, more generally, information from individual grid-cells should always be looked at in context with their broader spatial fields. This is partially due to the spatial variations described above. Spatial variability (or “noise”), particularly when looking at model-based climate projections, arises also in gridded data when small scale processes are averaged over the full grid cell. As models represent the underlying surface slightly differently, they will not reproduce the same details of the climate processes. Particularly in the moisture fields, namely precipitation, this will lead to model-to-model differences, further affecting the spatial coherence. Therefore, maps in the CCKP offer the user the broader context of a climate field to allow for a better interpretation of the robustness of a grid-based measure of the climatology or of a signal of change. Geospatial presentations, maps, use a Web Mapping Service (WMS) to visualize data and indicators on a map service, as shown in **Figure 1**.

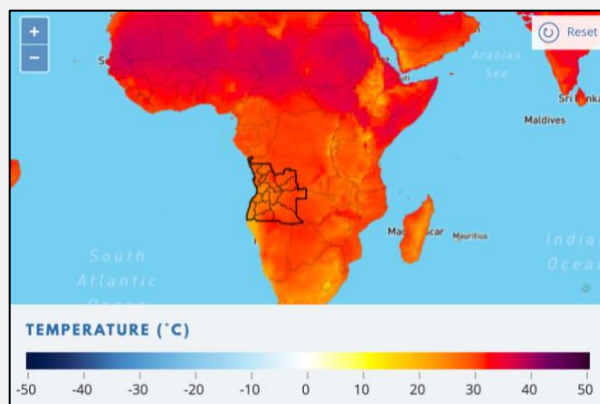


Figure 1. Observed, maximum temperature of Angola for the latest climatology, 1991-2020)

Observed data for the latest climatology, 1991-2020, is presented using the Köppen-Geiger Climate Classifications to support broader conceptualization of current climate contexts for a specific area (**Figure 2**). Underlying data for this presentation is CRU and calculations follow identified Köppen-Geiger classification methodology. Data and is presented at 0.5°x0.5° spatial resolution. For more information on Köppen-Geiger Climate Classifications, see [here](#).

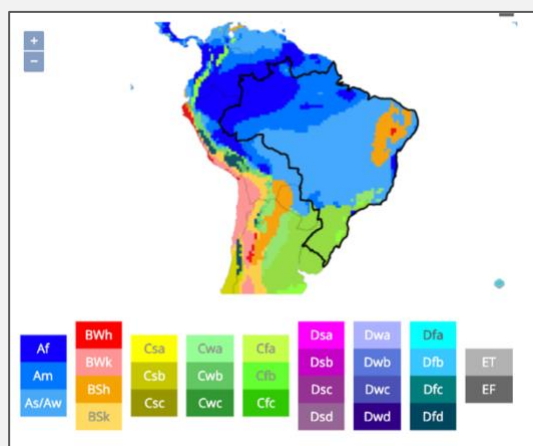


Figure 2. Köppen-Geiger Climate Classifications of Brazil for the latest climatology, 1991-2020)

Seasonal Cycle

The seasonal cycle enables precipitation and temperature data to be charted to illustrate seasonality for a defined climatology. **Figure 3a** shows seasonal cycle for the latest climatology, 1991-2020, presenting observational data for mean, min, max-temperatures and precipitation. **Figure 3b** shows projected maximum temperature anomaly across the seasonal cycle, this can be compared to the projected mean, which is presented in relation to the Historical Reference Period (**Figure 3c**). The shading area presents the range of model outputs, with the 10th and 90th percentiles and median (solid blue line).

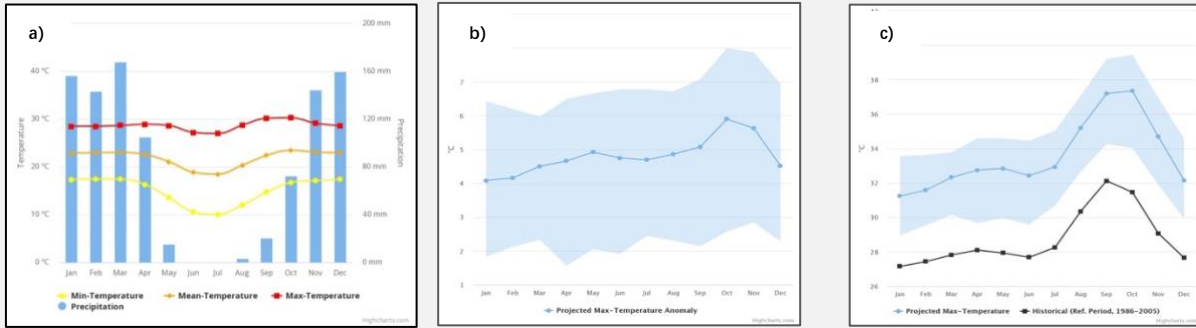


Figure 3. Seasonal cycle showing (a) the current climatology for observed data; (b) projected anomaly; (c) projected mean in relation to the historical reference period

Time Series

Time series provide insight into longer-term trends. **Figure 4a** shows the historical time series of the observed annual average temperatures, 1901 to 2020 with a smoothed trendline. **Figure 4b** shows the projected climatological average for mean temperature for each RCP, including the range of model outputs with median, 10th and 90th percentile.

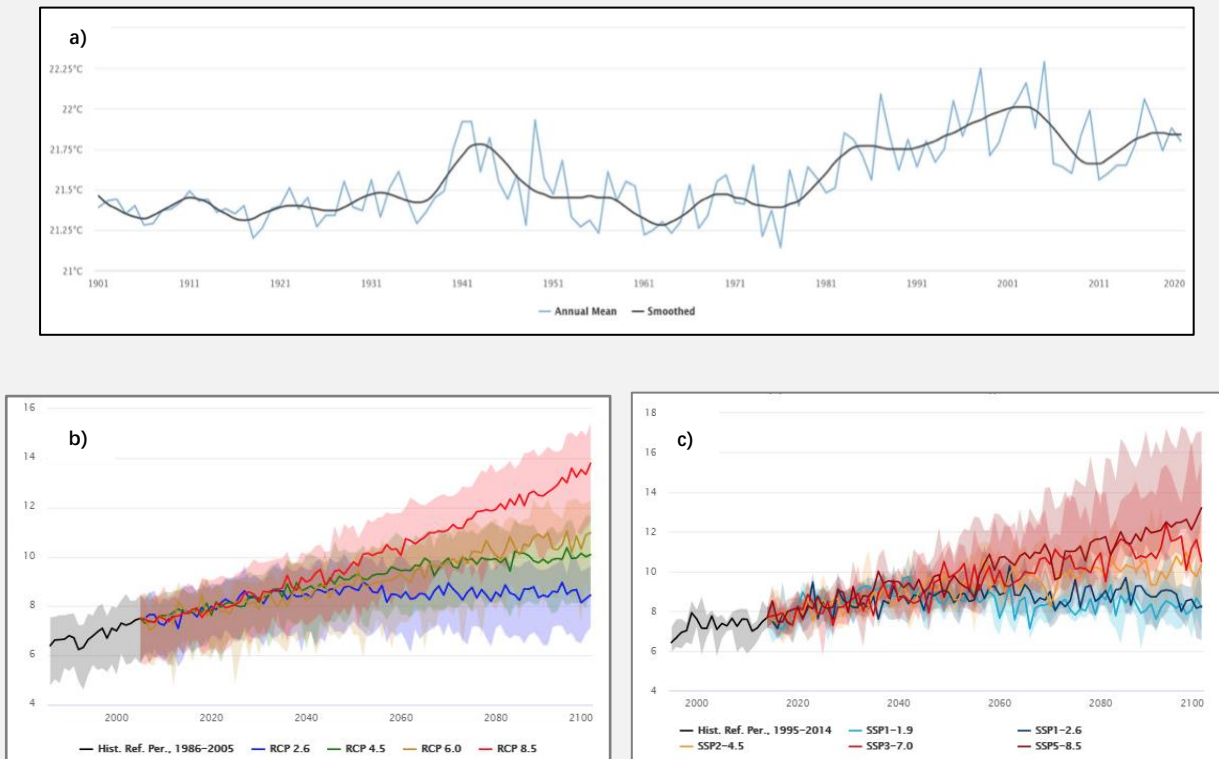


Figure 4. Time series presenting observed data (a); projected data across each RCP(b) and SSP(c)

Heatplot

The heatplot shows seasonal anomalies across longer-term time horizons. CCKP heatplots are created using CMIP5 projection data, with historical simulations from 1951 and projections through the end of the century. Monthly data is averaged across each ten-year period from 1951 to 2100. **Figure 5** shows the emerging seasonal anomalies of Tropical Nights for September to April increasing in magnitude from the 2050s.

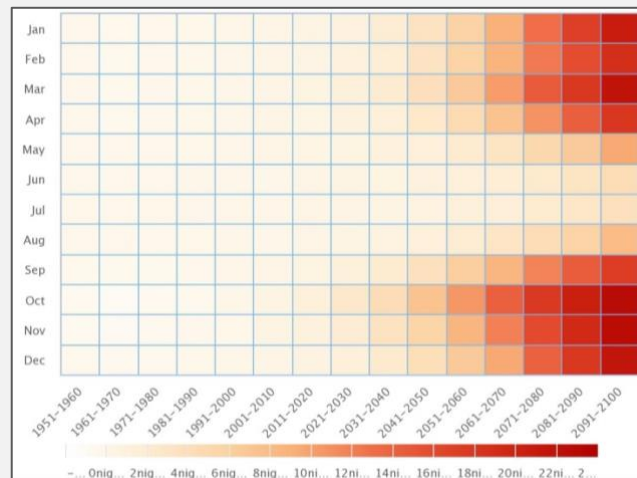


Figure 5. Heatplot presenting Tropical Night ($T_{min} > 20C$) anomalies, RCP8.5

2. VULNERABILITY

NATURAL HAZARDS DATA

Datasets: Tropical cyclone, Storm surge, Earthquake, Volcanic eruption, Tsunami, Flood

Credits: UNISDR Global Assessment Report (2015) Risk Platform. The global assessment report 2015 is based on a joint effort by leading scientific institutions, governments, agencies and development banks, the private sector and non-governmental organizations. The CAPRA software used for visualization was developed by UNISDR in collaboration with the world bank, CIMNE, ERN and INGENIAR, with the generous financial support of the European Commission.

Link: <https://preview.grid.unep.ch/>
<https://www.preventionweb.net/understanding-disaster-risk/graf>

Description: In the UNISDR-led assessment, probabilistic hazard models have been developed for earthquake, tropical cyclone wind and storm surge, tsunami and river flooding worldwide, for volcanic ash in the Asia-pacific region and for drought in parts of Africa. The probabilistic hazard models were later used to inform the global risk model for each hazard type. The datasets and methods used to calculate probabilistic hazard is different for each hazard type. The return periods selected to be represented in the CCKP is different for each hazard. Global cyclone hazard data measured as wind speed that is expected to be exceeded at least once in a 100-year mean return period. Global storm surge hazard data measured as inundation height that is expected to be exceeded at least once in a 10-year mean return period. Global earthquake hazard data measured as ground motion intensity (PGA) that is expected to be exceeded at least once in a 475-year mean

return period. Global tsunami hazard data which is expected to occur at least once in 500-year mean return period. Global flood hazard data measured as inundation height that is expected to be exceeded at least once in 100-year mean return period. More information and metadata/credits specific to each hazard type can be found [here](#).

GLOBAL RISK DATA PLATFORM

Datasets: Wildfire, Drought, Earthquake-induced Landslides, Rainfall-induced Landslides

Credits: GIS processing UNEP/UNISDR

Link: <http://preview.grid.unep.ch/index.php?preview=data&lang=eng>

Description: The Global Risk Data Platform is a multiple agencies effort to share spatial data information on global risk from natural hazards. Users can visualize, download or extract data on past hazardous events, human & economical hazard exposure and risk from natural hazards. It covers tropical cyclones and related storm surges, drought, earthquakes, biomass fires, floods, landslides, tsunamis and volcanic eruptions. The collection of data is made via a wide range of partners (see About for data sources). This was developed as a support to the Global Assessment Report on Disaster Risk Reduction (GAR) and replace the previous PREVIEW platform already available since 2000. Many improvements were made on the data and on the application. More information and metadata/credits specific to each hazard type can be found [here](#).

PACIFIC ISLANDS HAZARDS

Datasets: Earthquake, Tropical Cyclone (for a selection of Pacific Islands)

Credits: PCRAFI - PCRAFI is a joint initiative of SOPAC/SPC, World Bank, and the Asian Development Bank with the financial support of the Government of Japan and the Global Facility for Disaster Reduction and Recovery (GFDRR), and technical support from AIR Worldwide, NZ GNS Science, Geoscience Australia, Pacific Disaster Center (PDC), OpenGeo and GFDRR Labs

Link: <http://pcrafi.sopac.org/>

Description: The Pacific Catastrophe Risk Assessment and Financing Initiative (PCRAFI) aims to provide the Pacific Island Countries (PICs) with disaster risk modeling and assessment tools. PCRAFI produced detailed probabilistic hazard models for all 15 countries, such as Tropical Cyclones with Winds, Storm Surge, Rain Earthquake with Ground-shaking, and Tsunami. The information displayed on the CCKP are earthquake hazard data measured as ground motion intensity (PGA) that is expected to be exceeded at least once in 100-year mean return period, and tropical cyclone hazard data measured as wind intensity that is expected to be exceeded at least once in 100-year mean return period. More information and metadata/credits specific to each hazard type can be found [here](#).

EM-DAT

Datasets: Top disasters, Number killed, Number of affected, Average annual disaster occurrence by type.

Credits: EM-DAT: The OFDA/CRED International Disaster Database – www.emdat.be – Université Catholique de Louvain – Brussels – Belgium.

Public Database: <https://public.emdat.be>

Description: EM-DAT contains essential core data on the occurrence and effects of over 18,000 mass disasters in the world from 1900 to present. The database is compiled from various sources, including UN agencies, non-governmental organizations, insurance companies, research institutes and press agencies.

3. IMPACTS

AGRICULTURE

LOW/HIGH INPUT, IRRIGATED/RAINFED CROPS

Credits: Fischer, G., Nachtergaele, F.O., Prieler, S., Teixeira, E., Toth, G., van Velthuisen, H., Verelst, L., and Wiberg, D. (2012). Global Agro-ecological Zones (GAEZ v3.0)- Model Documentation. IIASA, Laxenburg, Austria and FAO, Rome, Italy., Laxenburg, Austria; Rome, Italy.

Links: <http://www.fao.org/soils-portal/soil-survey/soil-maps-and-databases/harmonized-world-soil-database-v12/en/>

<http://pure.iiasa.ac.at/id/eprint/13290/>

Description: The datasets provided under this contract were calculated with the latest version of AEZ programs (termed GAEZ v3.0) being published by IIASA and FAO. The files prepared for download on 10 June 2016 represent additions and a partial update of files provided to the World Bank's Climate Change Team.

GLOBAL IRRIGATED AREAS MAP

Credits: IWMI, [View Full Credits](#)

Description:

This is the version 2.0 release (update; as of May 10, 2007) of the International Water Management Institute's (IWMI's) Global irrigated area map (GIAM) and associated products and data. The GIAM products are produced using time-series data of: (a) AVHRR 10-km monthly from 1997-1999, (b) SPOT 1-km monthly for 1999, (c) GTOPO30 1-km elevation, (d) CRU 50-km grid monthly precipitation from 1961-2000, (e) AVHRR derived 1-km forest cover, and (f) AVHRR 10-km skin temperature. In addition, JERS SAR data was used for the African and South American rainforests.

There are many unique features in the IWMI's GIAM product line. First, this is the very first satellite sensor based global irrigated area map. Second, the resolution of the map (10-km) is the best that is presently available for irrigated areas at global level. Third, the area calculations are done for each season. So, the area irrigated at the end of the last millennium for the entire world was: (a) 257 Mha during June-September, (b) 174 Mha during October-February, and (c) 41 Mha during March-May. Further, there is a flexibility to calculate areas every month. Fourth, this is NOT just a map. There exists a suite of products that consists of maps, images, class characteristics, area calculations, snapshots and photos, animations, and accuracies. There are numerous advantages of such a product line. For example, disaggregated class images can be downloaded, and a more refined map can be created with local expertise for one's area of interest. The irrigated areas are used to create 20-year animations using AVHRR monthly time-series, so that one can spatially re-create the history of an irrigated area class. The class characteristics facilitate deriving crop calendar, sowing-peak-harvest dates of each class, and determine whether a class is single, double, or continuous crop. Fifth, the study develops and/or adopts a suite of innovative methods and techniques to map irrigated areas of the World at Global to local

levels and at all resolutions or scale. The methods include spectral matching techniques (SMTs), image segmentation, decision tree algorithms and spatial modeling, data fusion, space-time spiral curves, brightness-greenness-wetness 2-dimensional feature space plots, NDVI time series plots, NDVI thresholds, principal component analysis, and unsupervised clustering algorithms. The wide array of ground truth data was also used. This included ground truth data of the Indus-Ganges river basins, Krishna river basin, IWMI's ground truth data of the World that included data for Middle East and Africa, the degree confluence project data of the world, and the 150-m Landsat geo-cover mosaic of the world.

GLOBAL MAP OF RAINFED CROPLAND AREAS

Credits: IWMI – water data

Link: <http://waterdata.iwmi.org/applications/giam2000/>

Description: THE IWMI'S GLOBAL MAP OF RAINFED CROPLAND AREAS (GMRCA) is a by-product derived when working on IWMI's Global Map of Irrigated Areas (GMIA). The datasets approaches, and methods used to produce GMRCA are, to a great extent, similar to producing GIAM. Thereby, we refer the reader to detailed documentation on GIAM made available in this web site.

The Global Rainfed Croplands were estimated at 1.132 billion hectares at the end of the last millennium, from the GMRCA products (Biradar et al., 2007). This is 2.78 times the TAAI or net irrigated areas (407 Mha) of the World. The GMRCA area provided here is for the June–October period only. Like, GMIA it is possible to estimate seasonal Global Rainfed Cropland areas using the products and methods developed in this study. However, double crop rainfed is considered negligible. The total cropland is estimated as 1.539 billion hectares of which 1.13 billion rainfed and 0.407 irrigated.

The importance of rainfed croplands cannot be over-emphasized. Rainfed croplands meet about 60 percent of the food and nutritional needs of the World's population, are backbone of the marginal or subsistence farmers, and are increasingly seen as better alternative to irrigated agriculture as a result of its environmental friendliness and sustainability over long time periods. Rainfed agriculture has an history of roughly 10,000 years compared to about 6000-year history of irrigated agriculture (see World resources 1992-1999, and Mackenzie and Mackenzie, 1995). Literature shows that the World's croplands increased from about 265 million hectares in year 1700 to about 1.4 billion hectares in 1990, of which rainfed cropland alone is about 1.2 billion hectares (Cramer and Soloman, 1993, Richards, 1990, Grubler, 1994, World Resources 1992-1999). Our estimate of rainfed croplands of the World, at the end of the millennium, is 1.13 billion hectares.

Most global digital maps (e.g., Loveland et al. 1999, Olson and Watts, 1982, Matthews, 1983) overestimate agricultural areas as a result of the pixel-based area calculations (see Xiao, 1997, Cramer and Soloman, 1993). A pixel when classified as agriculture is automatically taken to have 100 % croplands in digital global maps. In reality only a certain percentage of a pixel is in cropland and that percentage can vary substantially. As a result the total agricultural lands estimated in various digital maps were 2.7 billion hectares by Olson and watts (1982) using a 50-km grid, 3.2 billion hectares by Matthews (1983) using 100-km grid, and 2.8 billion hectares by IGBP and USGS using 1-km grid (see Loveland et al. 1999). The FAO estimates based on Country statistics are closer to reality. The FAO statistics show cultivated areas at about 1.5 billion hectares (FAO, 2002). Grubler (1994) estimated that an increase of 1 billion arable lands would be needed for additional 5 billion world population in the 21st century.

The theoretical potential for cropland areas in the present climatic conditions and based on soil, climate, and topography are estimated at 3.29 billion hectares (Xiao et al. 1997) to 4.15 billion hectares (Cramer and Soloman, 1993). However, it must be noted that the productivity of a large proportion of these lands is limited

due to poor soil fertility, soil depth, access to water, and disease (e.g., Tse-tse flies and the black fleas). Any increase will have to come from land conversions from forests and rangelands which will be environmentally costly (Richards, 1990) or from protected areas which is unacceptable.

In reality, cropland areas are shrinking in recent times as a result of soil degradation, urbanization, and desertification and global warming. Between the early 1960s and the late 1990s, world cropland grew by only 11 percent, while world population almost doubled. As a result, cropland per person fell by 40 percent, from 0.43 ha to only 0.26 ha and reduced from 0.23 to 0.11 hectares (FAO, 2002). In future, 80 percent of increased crop production in developing countries will have to come from intensification: higher yields, increased multiple cropping and shorter fallow periods.

Thereby, tracking changes in spatial distribution and changing patterns of rainfed croplands is essential for understanding and planning food and nutritional demands of expanding populations of the World.

In this context, the IWMI's GMRCA product-line provides a benchmark measure of Rainfed Cropland Areas of the World at the end of the last millennium. The sub-pixel area (SPAs) of GMRCA provides realistic estimates of the actual area cultivated unlike the full pixel areas (FPAs) of almost all other studies. The GMRCA product-lines have maps, images, area characteristics and calculations, snapshots, and animations. In addition, the satellite sensor data mega-files and the ground-truth data used to produce the GMRCA are made available.

There are two product-lines within GMRCA. These are: (1) aggregated 9-class GMRCA map of the World; and (2) dis-aggregated 67-class GMRCA map of the World. The aggregated classes provide broad categories of rainfed cropland classes. Often, most users would just need such broad classes. The disaggregated classes provide a detailed picture and are often invaluable at regional, National, and local levels. For certain users, even at global level so that they can derive specific classes of interest to them. The class labeling in disaggregated classes are only indicative and can be improved.

GLOBAL MAP OF IRRIGATION AREAS

Credits: Stefan Siebert, Petra Döll, Sebastian Feick, Jippe Hoogeveen and Karen Frenken (2007) *Global Map of Irrigation Areas version 4.0.1*. Johann Wolfgang Goethe University, Frankfurt am Main, Germany / Food and Agriculture Organization of the United Nations, Rome, Italy. URL:

<http://drylandsystems.cgiar.org/content/irrigated-areas-0>

Link: <http://www.fao.org/nr/water/aquastat/irrigationmap/index10.stm>

Description: The latest version of the "Global Map of Irrigation Areas" is version 4.0.1. The map shows the amount of area equipped for irrigation around the turn of the 20th century in percentage of the total area on a raster with a resolution of 5 minutes. The area actually irrigated was smaller, but is unknown for most countries. A special note has to be made for Australia and India where the map shows the total area actually irrigated. This is due to the fact that statistics collected in Australia and India refer to actually irrigated area as opposed to statistics with area equipped for irrigation which are collected in most other countries. An explanation of the different terminology to indicate areas under irrigation is given in this glossary.

The map is generated as a grid and distributed with the following characteristics:

Projection:	Geographic
Number of columns:	4320
Number of rows:	2160
North Bounding Coordinate:	90 degrees
East Bounding Coordinate:	180 degrees

South Bounding Coordinate:	-90 degrees
West Bounding Coordinate:	-180 degrees
Cell Size:	5 minutes, 0.083333 decimal degrees
NODATA values:	Cells without irrigation are characterized by NODATA (-9), it does not mean that there was no data for these cells

For the GIS-users the map is distributed in two different formats: as zipped ASCII-grid that can be easily imported in most GIS-software that support rasters or grids; and, to accommodate people who use GIS-software that doesn't support rasters or grids, as a zipped ESRI shape file. It should be noted, however, that the values in the ASCII-grid have a precision of 6 decimals while the values in the shapefile have a precision of 2 decimals. For model calculations, it is therefore recommended to use the grid-version. As a service to those people who would need to know the absolute area equipped for irrigation, another ASCII-grid is available in which the area equipped for irrigation is expressed in hectares per cell. Non-GIS-users can download the map as PDF-file in two different resolutions.

HARVESTED AREA AND YIELDS (M3-CROPS DATA)

Credits: Monfreda et al. (2008), "Farming the planet: 2. Geographic distribution of crop areas, yields, physiological types, and net primary production in the year 2000", Global Biogeochemical Cycles, Vol.22, GB1022, doi: <https://doi.org/10.1029/2007GB002947>

Description: Described in the publication, Monfreda et al. (2008), "Farming the planet: 2. Geographic distribution of crop areas, yields, physiological types, and net primary production in the year 2000", Global Biogeochemical Cycles, Vol.22, GB1022, doi:10.1029/2007GB002947. The data is provided in NetCDF and ArcGIS ASCII format at 5-minute resolution in latitude by longitude. The NetCDF files have 4 levels (ArcGIS files only have the 1st two levels; contact authors if you want the other two levels), as follows: Level 1 = Harvested Area (unit = proportion of grid cell area). Note that values can be greater than 1.0 because of multiple cropping. Level 2 = Yield (unit = tons per ha). Levels 3 and 4 = Administrative levels from which the source data in levels 1 and 2 come from respectively. In levels 3 and 4, a value of 1 = county; .75 = state; .5 = interpolated from within 2 degrees lat/long; .25 = country; 0 = missing.

WATER

WATER INDICATOR

Datasets: Flood Indicator, Drought Indicator, Mean Annual Runoff, Annual Base Flow, Storage, Mean Annual Irrigation Deficit

Credits: Strzepek, K., McCluskey, A., Boehlert, B., Jacobsen, M., & Fant IV, C. (2011). *Climate Variability and Change: A Basin Scale Indicator Approach to Understanding the Risk to Water Resources Development and Management*. The World Bank.

Link: http://www.un.org/waterforlifedecade/pdf/2011_world_bank_climate_variability_change_eng.pdf

Description: This study evaluates the effects of climate change on six hydrological indicators across 8,413 basins in World Bank client countries. These indicators—mean annual runoff (MAR), basin yield, annual high flow, annual low flow, groundwater (baseflow), and reference crop water deficit—were chosen based on their relevance to the wide range of water resource development projects planned for the future. To generate a robust, high-resolution understanding of possible risk, this analysis examines relative changes in all variables from the historical baseline (1961 to 1999) to the 2030s and 2050s for the full range of 56 General Circulation

Model (GCM) Special Report on Emissions Scenario (SRES) combinations evaluated in the Intergovernmental Panel on Climate Change (IPCC) Fourth Assessment Report (AR4).

AQUASTAT

Credits: FAO

Link: <http://www.fao.org/nr/water/aquastat/main/index.stm>

Description: AQUASTAT is FAO's global information system on water and agriculture, developed by the Land and Water Division. The main mandate of the programme is to collect, analyze and disseminate information on water resources, water uses, and agricultural water management with an emphasis on countries in Africa, Asia, Latin America and the Caribbean. This allows interested users to find comprehensive and regularly updated information at global, regional, and national levels.

In AQUASTAT, three types of water withdrawal are distinguished: agricultural, municipal (including domestic), and self-abstracted industrial water withdrawal. A fourth type of anthropogenic water use is the water that evaporates from artificial lakes or reservoirs associated with dams. Information on evaporation from artificial lakes will be available in the AQUASTAT database in the near future.

At global level, the withdrawal ratios are 70 percent agricultural, 11 percent municipal and 19 percent industrial. These numbers, however, are biased strongly by the few countries which have very high-water withdrawals. Averaging the ratios of each individual country, we find that "for any given country" these ratios are 59, 23 and 18 percent respectively.

For Africa, Asia, Latin America and the Caribbean, AQUASTAT obtains water withdrawal values from ministries or other governmental agencies at a country level, although some data gaps are filled from UN Data. For Europe and for Northern America, Japan, Australia and New Zealand, Eurostat and OECD are valuable sources of information, and also used to fill data gaps.

SEA LEVEL

HISTORICAL SEA LEVEL ANOMALY

Data source: ESA, CLS, LEGOS, NOC, TUM. DOI: 10.5270/esa-sea_level_cci-MSLA-1993_2015-v_2.0-201612
<https://climate.esa.int/en/projects/sea-level/data/>

Historical Sea Level Anomaly (SLA) is defined as the height of water over the mean sea surface in a given time and region. This dataset contains monthly global sea surface height products from satellite observations. These data were produced at CNES as part of the European Space Agency's (ESA) Sea Level Climate Change Initiative (CCI) project. It contains a multi-satellite merged time series of monthly gridded Sea Level Anomalies (SLA) which has been produced from satellite altimeter measurement. This dataset is available at spatial resolution of 1/4 degrees lat/lon in Cartesian grids projection. The products are stored using the NetCDF format and CF (Climate and Forecast) metadata conventions. The way CF conventions are applied to ECV products with specific CCI additional vocabularies is defined in the frame of CCI Data Standards Working Group (DSWG).

It is important to note that the global sea level anomaly product was developed for open ocean applications and not coastal adaptation. Its interpretation and use in the coastal zone should therefore be done with caution. It is recommended to combine the product with in-situ (local) and regional model data to better estimate coastal sea level rise for adaptation purposes. The spatial patterns of anomalies at any given point in time are strongly influenced by local winds, water temperatures and ocean circulation (including large scale

features such as ENSO, for example). These localized features change on a daily, weekly, monthly, annual and/or decadal basis. Therefore, anomalies over a short time interval are exhibiting very noisy spatial patterns. Long-term trends can only be recognized in longer timeseries.

Data Processing:

1. Land Masking

Due to the resolution of the raw Sea Level Anomaly data, parts of the dataset overlap with land. To remove the data over land, the following process was applied:

- a. The resolution of each image was up-sampled to have a resolution of 1km x 1km;
- b. Each image was clipped using a land-mask based on the Open Street Map Data Land polygons dataset¹ such that the sea level anomaly data would be at most 1km from land; and
- c. Each image was compressed and projected to EPSG:3857 (web Mercator) to overlay on Google Maps in the Climate Change Knowledge Portal.

2. Creating Country-level Data

In discussion with the World Bank, it was determined that Sea-Level Anomaly data assigned to a country and made available in a Data API should be displayed in graph or tabular form in the Climate Change Knowledge Portal only at a country's coastline.

It is important to note that the global sea level product was developed for open ocean applications and not coastal adaptation. Its interpretation and use in the coastal zone should therefore be taken with caution. It is recommended to combine the product with local in situ and regional model data to better estimate coastal sea level rise for adaptation purposes.

To extract sea level anomaly information at the coast, a custom processing tool has been created. To process data for each country, the following processing chain is followed:

- a. Retrieve Web Coverage Service (WCS) online resource stored in the EO4SD CR platform for the Sea Level Anomaly datasets, sub-setting the data on-the-fly using the country borders file provided by the World Bank;
- b. For each date in the Time of Interest interval, country-aggregated sea level rise values are stored in a database structure;

OBSERVED SEA SURFACE TEMPERATURE

Data Origin: Merchant, C.J., Embury, O., Bulgin, C.E., Block T., Corlett, G.K., Fiedler, E., Good, S.A., Mittaz, J., Rayner, N.A., Berry, D., Eastwood, S., Taylor, M., Tsushima, Y., Waterfall, A., Wilson, R., Donlon, C. Satellite-based time-series of sea-surface temperature since 1981 for climate applications, *Scientific Data* 6:223 (2019). <http://doi.org/10.1038/s41597-019-0236-x>

Data Service: Good, S.A.; Embury, O.; Bulgin, C.E.; Mittaz, J. (2019): ESA Sea Surface Temperature Climate Change Initiative (SST_cci): Level 4 Analysis Climate Data Record, version 2.1. Centre for Environmental Data Analysis, 22 August 2019. doi: <http://dx.doi.org/10.5285/62c0f97b1eac4e0197a674870afe1ee6>

Data Access: <https://climate.esa.int/en/projects/sea-surface-temperature/>

This product is the Level 4 Sea Surface Temperature (SST) Analysis data produced by the ESA Climate Change Initiative (CCI). It consists of daily, spatially complete (gap filled) estimated SST data, derived using the

Operational Sea Surface Temperature and Sea Ice Analysis (OSTIA) processing system. It combines data from both the Advanced Very High-Resolution Radiometer (AVHRR) and Along Track Scanning Radiometer (ATSR) SST_cci Climate Data Records, using a data assimilation method to provide SSTs where there were no measurements.

Time Aggregations: The original ESA CCI SST data at daily resolution on a 0.05 degrees grid are aggregated to monthly averages to align with the temporal resolution of other climate-related variables. For the same reason, the spatial resolution of monthly data has been degraded to 0.25 degrees.

Creating Country-level Data: It is important to note that the SST product was developed for open ocean applications and not coastal adaptation. Its interpretation and use in the coastal zone should therefore be taken with caution. It is recommended to combine the product with local in situ and regional model data to better estimate coastal sea surface temperature for adaptation purposes.

To extract SST information at the coast, a custom processing tool has been created using the original SST data (daily, 0.05 degree resolution). To process data for each country, the following processing chain is followed:

- a. Retrieve Web Coverage Service (WCS) online resource stored in the EO4SD CR platform for the SST datasets, sub-setting the data on-the-fly using the country borders file provided by the World Bank;
- b. For each date in the Time of Interest interval, country-aggregated SST values are stored in a database structure;

SEA LEVEL RISE PROJECTS

Data Service: Integrated Climate Data Center - ICDC/ University of Hamburg

<https://icdc.cen.uni-hamburg.de/ar5-slr.html>

Processing methods and data sources are explained in AR5 Sea Level Change Supplementary Material, Chapter 13: https://www.ipcc.ch/site/assets/uploads/2018/07/WGI_AR5.Chap_13_SM.1.16.14.pdf

Sea level rise (SLR) is the sum of oceanic thermal expansion, ice melt from glaciers and small ice sheets, melt and ice loss from Greenland and Antarctica, and changes in terrestrial water storage. SLR is accelerating in response to climate change and is producing significant impacts already being felt by coastal ecosystems and communities. SLR and other oceanic climate change will result in salinization, flooding and erosion and affect human and ecological systems, including health, heritage, freshwater, biodiversity, agriculture, fisheries and other services. Increased heat in the upper layers of the ocean is also driving more intense storms and greater rates of inundation, which, together with SLR, are already driving significant impacts to sensitive coastal and low-lying areas. By the end of the 21st century, it is very likely that sea level will rise in more than about 95% of the ocean area and about 70% of the coastlines worldwide are projected to experience a sea level change within $\pm 20\%$ of the global mean.¹²

¹² IPCC, 2018: *Global Warming of 1.5°C. An IPCC Special Report on the impacts of global warming of 1.5°C above pre-industrial levels and related global greenhouse gas emission pathways, in the context of strengthening the global response to the threat of climate change, sustainable development, and efforts to eradicate poverty* [Masson-Delmotte, V., P. Zhai, H.-O. Pörtner, D. Roberts, J. Skea, P.R. Shukla, A. Pirani, W. Moufouma-Okia, C. Péan, R. Pidcock, S. Connors, J.B.R. Matthews, Y. Chen, X. Zhou, M.I. Gomis, E. Lonnoy, T. Maycock, M. Tignor, and T. Waterfield (eds.)]. URL: <https://www.ipcc.ch/sr15/download/>

The AR5 SLR data were used in the construction of figures for the Fifth Assessment Report of the Intergovernmental Panel on Climate Change (IPCC-AR5). The data include 10 geophysical sources that drive long-term changes in relative Sea Surface High (SSH):

- 5 ice components (Greenland dynamic ice and surface mass balance, Antarctic dynamic ice and surface mass balance, and glaciers),
- 3 ocean-related components, all of which are derived from CMIP5 models (dynamic SSH, global thermosteric SSH anomaly, and the inverse barometer effect from the atmosphere),
- land water storage (also called terrestrial water),
- and glacial isostatic adjustment (as a change in sea level relative to land).

SLR data are presented for three different RCP scenarios: 2.6, 4.5, 8.5.

Data Processing:

1. Creating Country-level Data

The CCKP presents this product in form of a global map and as time series averaged along the coastline of countries to illustrate ongoing changes. The SLR projection values are shown as deviations from the mean value over 1985-2005. It is important to note that the global sea level rise product was developed for open ocean applications and not coastal adaptation. Its interpretation and use in the coastal zone should therefore be taken with caution. It is recommended to combine the product with local in situ and regional model data to better estimate coastal sea level rise for adaptation purposes.

To extract sea level rise information at the coast, a custom processing tool has been created. To process data for each country, the following processing chain is followed:

- a.** Retrieve Web Coverage Service (WCS) online resource stored in the EO4SD CR platform for the Sea Level Rise datasets, sub-setting the data on-the-fly using the country borders file provided by the World Bank;
- b.** For each date in the Time of Interest interval, country-aggregated sea level rise values are stored in a database structure;